SANDIA REPORT
SAND2004-5970
Unlimited Release
Printed December 2004

Development of the Resin Infusion between Double Flexible Tooling Process – Assessment of the Viability of In-Mold Coating and Implementation of UV Curing

Dr. O.I. Okoli
Assistant Professor
Dept. Of Industrial & Manufacturing Engineering
FAMU-FSU College of Engineering
2525 Pottsdamer Street
Tallahassee, FL 32310-6046 USA

Prepared by Sandia National Laboratories
Albuquerque, New Mexico 87185 and Livermore, California 94550

Sandia is a multiprogram laboratory operated by Sandia Corporation,
a Lockheed Martin Company, for the United States Department of Energy's
National Nuclear Security Administration under Contract DE-AC04-94AL85000.

Issued by Sandia National Laboratories, operated for the United States Department of Energy by Sandia Corporation.

Available to DOE and DOE contractors from
U.S. Department of Energy
Office of Scientific and Technical Information
P.O. Box 62
Oak Ridge, TN 37831

Telephone: (865)576-8401
Facsimile: (865)576-5728
E-Mail: reports@adonis.osti.gov
Online ordering: http://www.osti.gov/bridge

Available to the public from
U.S. Department of Commerce
National Technical Information Service
5285 Port Royal Rd
Springfield, VA 22161

Telephone: (800)553-6847
Facsimile: (703)605-6900
E-Mail: orders@ntis.fedworld.gov
Online order: http://www.ntis.gov/help/ordermethods.asp?loc=7-4-0#online

SAND2004-5970
Unlimited Release
Printed December 2004

Development of the Resin Infusion between Double Flexible Tooling Process – Assessment of the Viability of In-Mold Coating and Implementation of UV Curing

Sponsored by the Sandia National Laboratories LDRD Program

Prepared by:
Dr. O. I. Okoli
Assistant Professor
Dept. Of Industrial & Manufacturing Engineering
FAMU-FSU College of Engineering
2525 Pottsdamer Street
Tallahassee, FL 32310-6046
USA

Abstract

As composites gain wider acceptance in all sectors of the economy, new methodologies must be developed to increase their cost effectiveness in manufacturing. The neoteric Resin Infusion between Double Flexible Tooling (RIDFT) process is undergoing modifications to improve its cost-effectiveness by developing methodologies for in-mold coating and the incorporation of UV curing.
In-mold coating is desired by the composites industry since it eliminates the current paint process, which is not only laborious and time consuming, but expensive, and presents safety issues. Two methodologies (paint films and coinfusion) for implementing in-mold coating were investigated. It was demonstrated that thermoform-

able paint films could be used to produce coated RIDFTed components. Coinfusion was also successfully implemented.

This work also investigated the feasibility of designing and incorporating a Cure on Demand system into the RIDFT process, using ultraviolet (UV) light for the curing of composite laminates. The objective was to develop a process for the RIDFT that would eliminate or reduce the inflexibility in the current production process, resulting in shortened production cycle times. UV-cured laminates were produced at a fraction of the time required to produce catalyst-cured laminates. Mechanical and material characterization tests were performed on each of the UV-cured laminates produced. The results were referenced against those obtained for laminates produced using a catalyst curing system to determine their overall quality. The UV-cured laminates, after undergoing tensile and rheological thermal tests, were found to have mechanical and material properties comparable, or in a few instances slightly better, than that of thermally cured laminates.

Acknowledgments

The author would like to extend his appreciation to the Sandia National Laboratories LDRD (Laboratory Directed Research and Development) program for funding this work and to Dr. Judith “Heidi” Ruffner for supporting our efforts at the Florida Advanced Center for Composites Technologies.

The hard work of the students that were involved in this project (Nicholas Toro, Posen Chiu, and Augustine Nwabuzor) is greatly appreciated.

This page intentionally left blank.

Contents

Figures

Tables

This page intentionally left blank.

Nomenclature

AHK	alpha hydroxyl ketone oxide
BAPO	(2,4,6-trimethylbenzoyl)-phosphine oxide
CIRTM	coinfusion resin transfer mold
CONAP	cobalt naphthalate
DMA	dynamic mechanical analysis
DoE	design of experiments
ESEM	environmental scanning electron microscope
IMC	in-mold coating
MEKP	methyl ethyl ketone peroxide
RIDFT	resin infusion between double flexible tooling
RTM	resin transfer molding
SMC	sheet molding compound
UV	ultraviolet
VaTRM	vacuum-assisted resin transfer molding

This page intentionally left blank.

1. Introduction

Over the past four decades, polymer composites have been regarded by many researchers as the material of the future due to their high strength to weight ratios, corrosion resistance, and functional integration [1]. However, the production economics of polymer composites tend to limit their application in the mass production sector. The lead times to manufacture are simply too high. Several production processes are available, with liquid composite molding techniques being the most amenable to mass production.

Techniques such as resin transfer molding (RTM), vacuum-assisted resin transfer molding (VaRTM), and their variants have been successfully implemented for the manufacture of polymer composite components. Once manufactured, composite components undergo a series of finishing processes to prepare the substrate for painting. Some of the current painting methodologies are not only laborious, time consuming, and expensive, but may also release materials that are harmful to the environment.

This work assessed the viability of manufacturing in-mold coated components using the neoteric Resin Infusion between Double Flexible Tooling (RIDFT) process developed at the Florida State University. The assessment of in-mold coating (IMC) was two-fold: by means of a thermoformable paint film, and by the coinfusion of the resin and coating materials. An assessment was also conducted to ascertain the viability of using UV lamps to cure photoinitiated resins for the rapid production of components using the RIDFT process.

This page intentionally left blank.

2. RIDFT Process

RIDFT was developed from a need to overcome mold filling and long production cycle time problems in manufacturing composite parts when using traditional RTM and VaRTM processes. The RIDFT concept vastly improves upon the processing procedure of traditional RTM/VaRTM processes. In this innovative process, the resin infusion and resin-fiber wetting is finished between two flexible tools in a two-dimensional, flat shape, and then the entire wetted reinforcement and flexible tooling is formed to a specified part shape by using vacuum. The production steps for the RIDFT process are shown in Figure 1 [2].

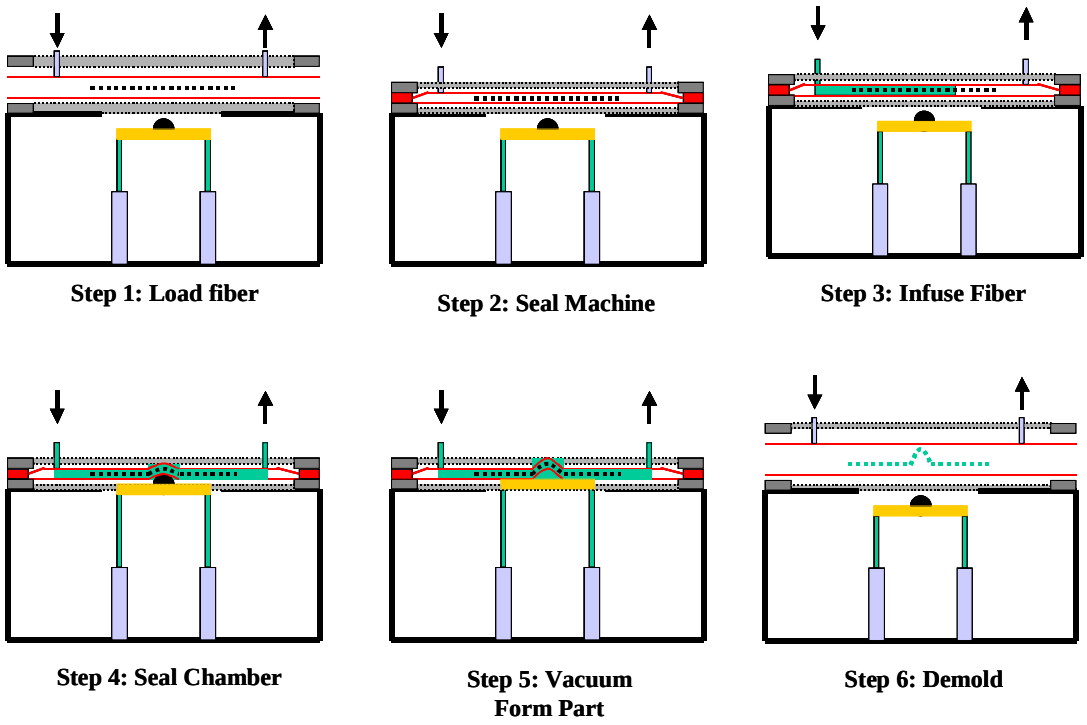

Figure 1. Schematic of the RIDFT process.

The first step of the process is to place dry fibers or fabrics onto the bottom layer of silicone rubber, which is directly over the mold. The fiber is precut to fit the desired shape to be formed. After carefully placing the fiber within the machine, the top layer of silicone is placed over the fiber and bottom layer of silicone, and then sealed around the edges. The sealed bag is kept in a flat panel shape. Next, the fiber lay-up between the two rubber layers is vacuum-infused using low viscosity resin. The vacuum chamber between the bottom rubber layer and mold setting cavity is sealed and a vacuum is pulled. This vacuum forces the silicone sheets with the wetted fibers or fabrics together to form over the shape of the mold. Finally, the cured part is removed from the RIDFT machine as a manufactured part.

With RIDFT, resin contact with the mold surface does not occur and eliminates the need to prepare the mold before each cycle; therefore, the cleanup and pre-manufacturing prep work is

reduced. In addition to reducing a manufacturing step, tool wear experienced from continuous use, as seen with the RTM process, is eliminated. Furthermore, because resin flows in a two-dimensional, flat shape, a number of flow-related problems in traditional RTM/VaRTM processes are avoided. Stacking or lay-up time for forming reinforcement into part shapes is saved and fiber preform applications in the process are not required.

3. In-Mold Coating

The automotive coatings market has been significantly influenced by the macroeconomic environment, the drive towards lower costs and higher efficiency, technology innovation, and sound environmental practice [3]. Environmental concerns have led the efforts to reduce solvent use in coating applications. The latest technology and materials development promise to lower assembly paint-line emissions, eventually eliminating solvents in paint, while improving scratch resistance and the overall durability of a vehicle finish.

In 2002, the worldwide market in automotive paints was worth $6.6 billion [3]. In the last few years, the U.S. market for automotive paint has seen a growth on average revenues of 1% above the rate of new car production, but volumes have fallen at a rate of 0.5% per year. This may be attributed to the deployment of more efficient coating equipment and paint with higher solid levels. It is imperative that methodologies are sought to reduce the costs associated with painting, as well as the negative environmental impacts. IMC of composite components may address these issues. IMC has been successfully used for many years for exterior body panels made from compression-molded, Sheet Molding Compound (SMC) to improve their surface quality in terms of functional and cosmetic properties [4]. When injected onto a cured SMC part, IMC cures and bonds to provide a paint-like surface [5]. Other methods for IMC are the use of thermoformable paint films and the coinfusion of coating materials.

3.1 In-Mold Coating Using Thermoformable Paint Films

The goal was to create a procedure for producing composite parts with a decorative finish to meet the customer's specifications. Similar processes have been previously developed, such as coating thermoforms and some two-step processes with thermosets, which have had some success in industry, but still hold many limitations. Developing a one-step forming and coating process should reduce processing time and associated costs, with obvious advantages to manufacturers.

This study utilizes Avery Dennison Avloy-film (AL10041g3.1525). The aim was to establish the variables that affect adhesion of the paint film to the part during the forming process. Reducing paint separation and improving the surface finish as much as possible is also important. The problem encountered was the accelerated curing of the vinyl ester resin when exposed to heat, which is necessary to sufficiently melt the paint film for proper adhesion. This reduces the time available for forming.

3.1.1 Procedure

Experimental assessments were carried out using the RIDFT prototype shown in Figure 2. The materials used were 7781 glass fibers with Derakane 470-45 vinyl ester resin. Six layers of glass fibers, cut to 6 inches × 5 inches, were used for each laminate. Surface veils were prepared for selected runs and cut to the same dimensions as the fibers. The fibers were placed on the bottom

silicone layer. When used, the surface veils were placed on the top fiber layer. The paint film was placed on the surface veil or the topmost fiber layer. The top silicone frame (Figure 3) was then placed, and the assembly sealed under a vacuum. The resin was catalyzed, assuring a suitable gel time. A mixture of 1% methyl ethyl ketone peroxide (MEKP) and 0.15% cobalt naphthalate (CONAP) was used for all experiments. Gel time at room temperature was between 50-60 minutes. Infusion was initiated within 20 seconds of the addition of the MEKP solution to the resin CONAP mixture. Approximately three minutes were allowed to elapse as fibers were completely infused. This time was consistent and only deviated by ± 20 seconds. Fiber infusion was completed before application of heat to allow for proper wetting. Time zero was set once infusion was completed, and all test parameters set by the designed experiment were set from this time. This means that the testing procedure was conducted in two phases. Phase one included wetting of fibers through infusion. This portion of the experiment took less than three minutes. The second phase began when all testing parameters were conducted.

Figure 2. RIDFT prototype.

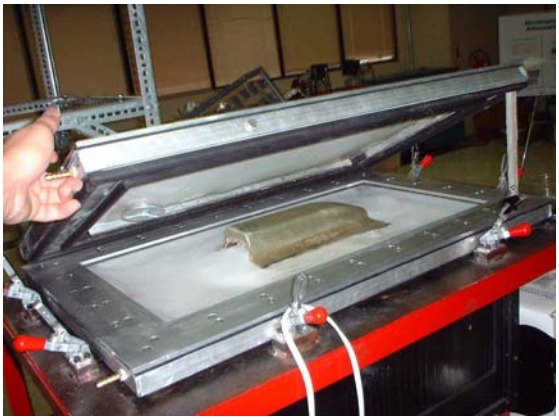

Figure 3. RIDFT prototype showing top and bottom sealing frames.

The effect of production variables, such as the temperature of the paint film, duration of heat application, and the use of a surface veil, on paint film adhesion, formability, and the resulting surface quality was investigated using design of experiments (DoE).

3.1.2 Design of Experiments

The DoE selected was a 2^{4-1} resolution IV with one center-point, which was doubled due to the categorical variable and surface veil application. This design provided information about the main effects and two factor interactions. It also assumes that all three-factor interactions can be neglected. This type of design provides a test for curvature, which may be a factor in some of the responses observed. It also required 10 runs to be performed, which addressed the limited resources such as time and material. If required, this experiment could be easily replicated to obtain an estimate of error, which was another consideration. The parameters and levels of each variable examined are included in Table 1.

Table 1. DoE parameters and associated levels (paint film)

Variables	High Level	Low Level
Lamp distance	5 inches	0 inches
Heat duration	3 minutes	0 minutes
Time of application	5 minutes	0 minutes
Use surface veil	No	Yes

These parameters were selected because earlier tests revealed that less than a one-minute window exists between the time the paint film is formable and the resin become rigid using the current 1% MEKP/0.15% CONAP to resin mixture, dependent on the temperature and duration of the heat applied. Table 2 shows the final response for each run.

3.1.2.1 Adhesion Response

The range of the response for examining paint film adhesion was set between 0 and 3. An explanation of this range is given below:

- 0 – No adhesion throughout part;
- 1 – No adhesion on some of the part;
- 2 – paint adhered, but air pocket remained;
- 3 – Compete adhesion, no air pockets.

The test runs that resulted in the best adhesion were those that were unable to form completely (Figure 4). On these parts, the paint film adhered fully. However, due to the increased temperatures resulting from the heat lamp and the curing resin, the part was unable to form and caused the paint film to blister, resulting in a very poor surface finish. Such effects were not expected, since the operating temperatures of the paint film were not exceeded with the lamp used. However, additional heat resulting from the curing resin may have increased the system's temperature.

The DoE (Figure 5) suggested that the lamp distance and heat duration significantly affects adhesion. All other parameters were not found to be significant.

Table 2. DoE response sheet with tabulated scores (paint film)

RUN	Distance	Application	Duration	Veil	Adhesion	Formability	S.F. Finish
1	5	5	2	yes	1.5	3	4
2	2.5	2.5	2.5	no	3	2	3
3	5	0	3	yes	2.5	2.25	2
4	0	5	3	yes	3	0	0
5	0	5	2	no	2.5	2.25	2
6	0	0	3	no	3	0	0
7	2.5	2.5	2.5	yes	2.5	1.2	3
8	5	0	2	no	2	2.9	4
9	0	0	2	yes	2.5	2.75	2
10	5	5	3	no	2.5	1.25	3

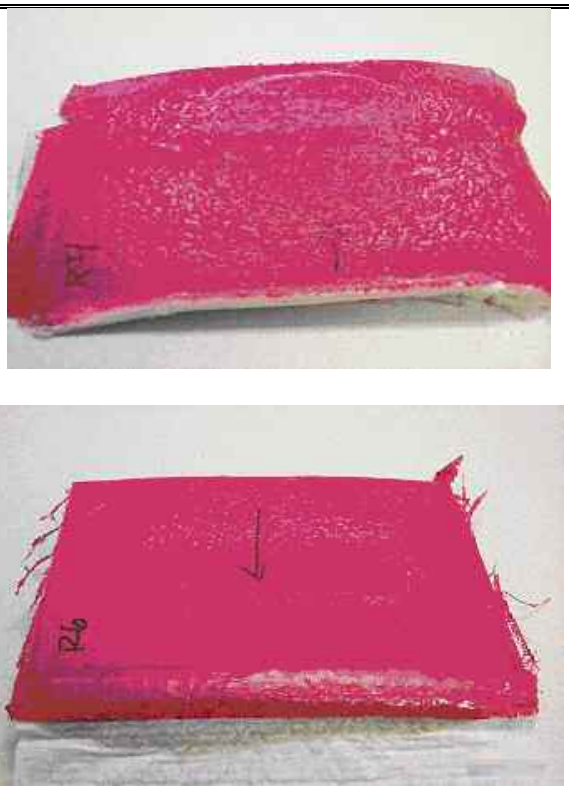

Figure 4. Surface finish of well-adhered part with blistering effect.

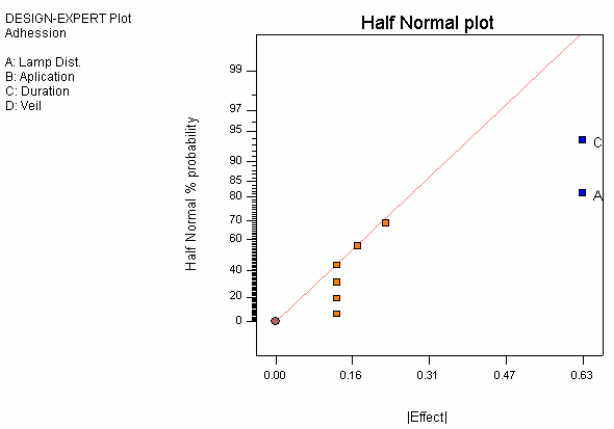

Figure 5. Half normal plot for adhesion.

3.1.2.2 Formability Response

A similar scheme to adhesion was created to measure formability. In this case, the responses varied from 0 to 2. A breakdown of the scheme can be explained as:

- 0 – Flat part obtained;
- 1 – Flared corners or edges; and
- 2 – Fully formed, perfect box.

Figures 6 and 7 show the flared corners and fully formed box, respectively. The half normal plot for this test (Figure 8) implied that only the lamp distance and heat duration were of significance.

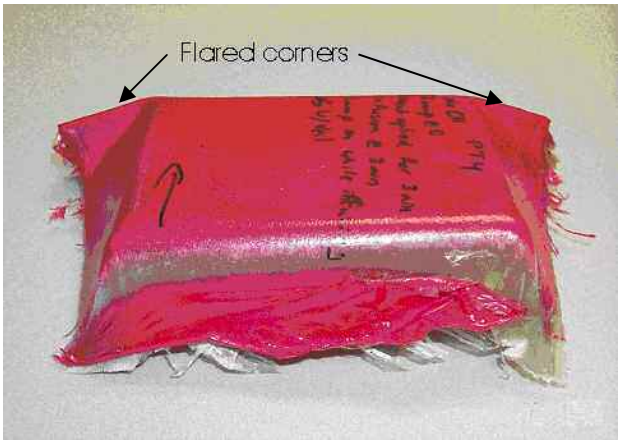

Figure 6. Part with flared corners.

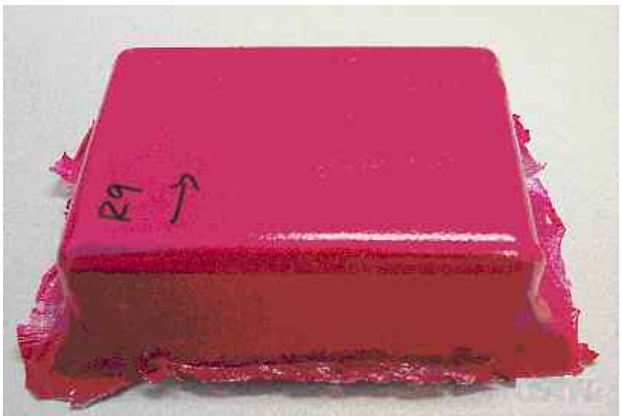

Figure 7. Part with perfect corners.

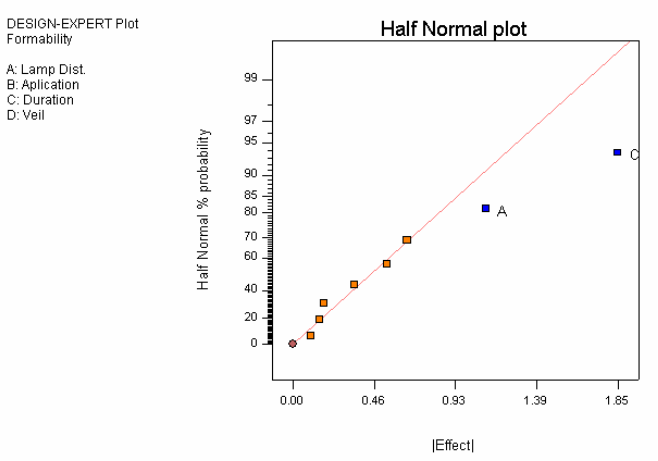

Figure 8. Half normal plot for formability.

3.1.2.3 Surface Finish Response

A similar scheme was used as with the previous responses. In this case, the responses ranged from 0 to 4, with 0 being low and 4 being high or optimum. The breakdown is given below:

- 0 – Paint separation, failure of paint film;
- 1 – Coarse print-through of fiber or surface veil (throughout entire part);
- 2 – Grainy print-through of fiber or surface veil (throughout entire part);
- 3 – Partial print-through (not throughout entire part); and
- 4 – No print-through, smooth surface.

There was one unexplained effect that involved the paint film becoming transparent. It appeared as if the paint separated at some locations (Figure 9). The results from the DoE (Figure 10) indicated that, as with the previous responses, the significant variables for surface finish were lamp distance and duration of heat exposure.

Figure 9. Part with paint separation.

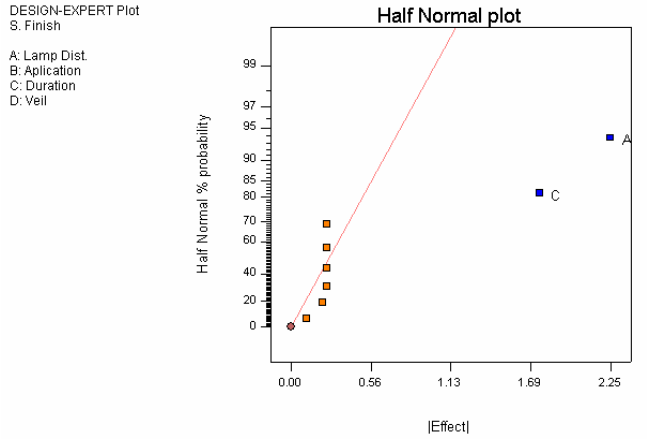

Figure 10. Half normal plot for surface finish.

3.1.3 Conclusion

This work intended to evaluate the viability of utilizing paint films as a means of IMC components produced by the RIDFT process. The results indicate that the heating duration and resultant temperature affected the paint quality. Furthermore, the temperature increase necessary for softening the paint films prematurely initiated curing, which impaired the formability of the fiber-resin assembly.

It was found that, although the current paint films did not adhere very well to the substrate, their inclusion did not affect resin flow. As such, it can be inferred that the use of an appropriate film with better adhesion characteristics will allow for the IMC of RIDFTed components. Further work is continuing, and paint films from other sources are being investigated.

3.2 In-Mold Coating by Means of Coinfusion

The goal was to create a procedure for producing composite parts with a decorative finish to meet the customer's specifications by coinfusing the resin and the coating material in a single process without opening the mold. The preliminary results of IMC assessment studies for RIDFTed components are presented here. A room-temperature cure vinyl ester resin was used with DuPont Imron 5000 paint.

3.2.1 Approach

Based on the work by Gillio et al. [6], a simplified schematic of the co-injection setup is shown in Figure 11. In the majority of cases, the flow of a polymer inside a mold filled with a stationary fiber bed was modeled using Darcy's law (Eqn. 1).

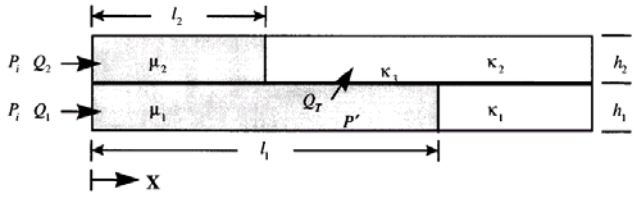

Figure 11. Schematic of the 1D flow model in coinfusion resin transfer mold (CIRTM) [6].

The macroscopic velocity, *u*, is given by

$$u = \frac{k}{\mu}\frac{dP}{dx}, \tag{1}$$

where *k* is the permeability of the fiber preform, μ is the viscosity of the resin, and *dp/dx* is the pressure gradient in the flow direction.

In coinjection, the top and the bottom preforms could have different permeabilities and the resins injected could have different viscosities, leading to different resin velocities between the top and the bottom halves of the mold. The injection is assumed to be at the same pressure, since this is the case in the majority of VaRTM type processes [6]. In such a case, the velocities of the two flow fronts will be given by

$$u_1 = \frac{k_1}{\mu_1}\frac{P_i}{l_1} \tag{2}$$

$$u_2 = \frac{k_2}{\mu_2}\frac{P_i}{l_2}. \tag{3}$$

The RIDFT set-up is illustrated in Figures 12 and 13.

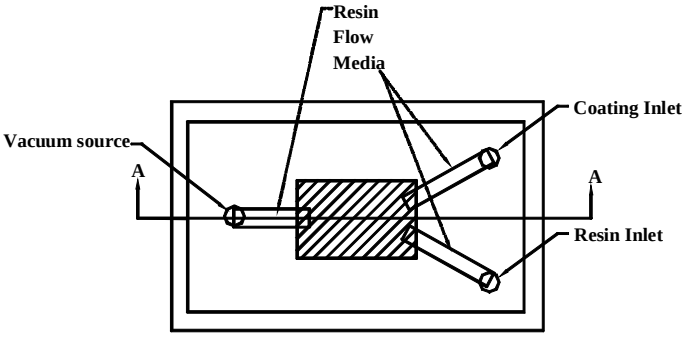

Figure 12. RIDFT IMC (Top view).

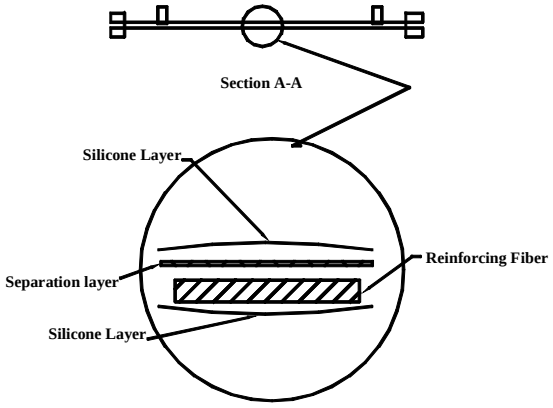

Figure 13. RIDFT IMC (Detailed).

The resin and coating material were infused through separate flow media under a vacuum (Figure 12). A layer of FERRO Prepak™ material separated the paint and resin to prevent mixing during infusion (Figure 13). The paint was infused first, followed by the resin, which dissolved the separation layer on contact.

3.2.2 Discussion of Results

A series of experiments were performed. Initial tests used an impermeable vacuum bag as the separation layer. The coating and the resin were coinfused successfully, demonstrating the viability of the experimental set-up (Figure 14). The bagging material was obviously unsuitable as a separation layer for IMC due to adhesive incompatibilities.

Other materials were assessed including the FERRO #MCO8 Prepak™ material. Initial infusion with coating and resin showed promise. However, since the coating material is more viscous than

the resin (30:1) and permeability $k_1 > k_2$ when infused concurrently, the resin filled the mold faster than the paint. Additionally, the resin depletes the separation material on contact (Figure 15). Therefore, it was necessary to first infuse the paint, then infuse the resin.

(a) (b)

Figure 14. (a) Top (coating) side of coinfused component; (b) Bottom (resin) side of component.

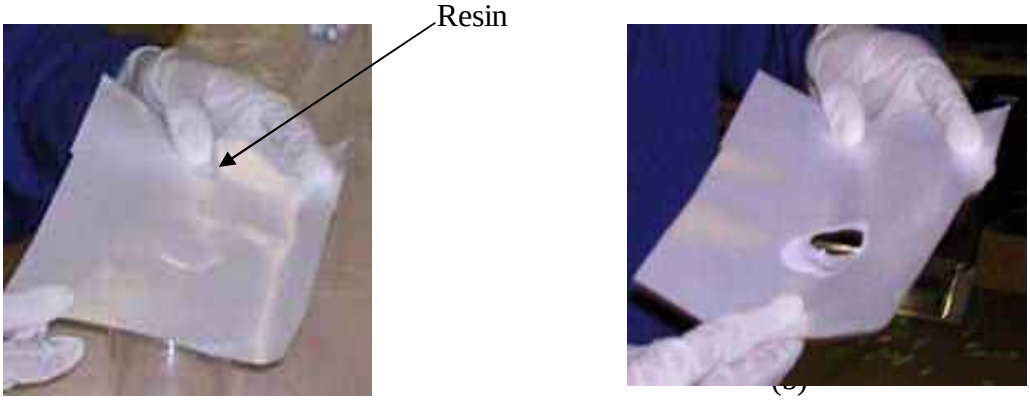

Figure 15. (a) Resin in contact with FERRO #MCO8 Prepak™ separation material; (b) Depletion of separation layer after three seconds

The separation layer was also found to be depleted by the coating material (Figure 16), although at a much slower rate than the resin. Nonetheless, the coating material depletion rate was enough to interfere with the integrity of the coinfused component. This is seen in Figure 17.

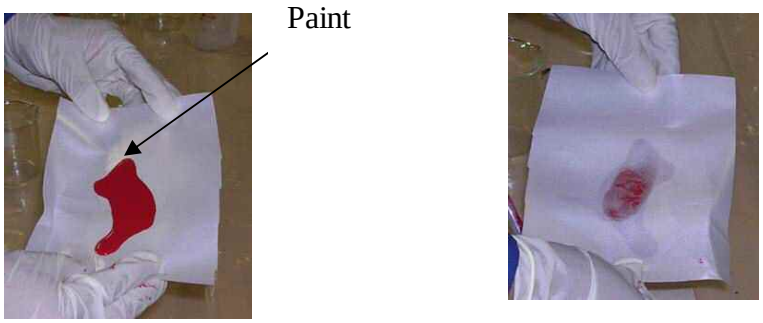

Figure 16. (a) Coating material in contact with FERRO #MCO8 Prepak™ separation material; (b) Depletion of separation layer after 60 seconds.

Figure 17. Paint percolation observed through the underside of the flexible RIDFT mold.

Figure 17 shows that the coating material was able to deplete the separation layer. This means that when the resin was infused, the flow was disturbed by the presence of the paint. This may have resulted in the paint interfering with the fiber-matrix interface. Figure 18 is the microstructure of a failed IMC specimen. It shows extensive fiber pullout, which is indicative of a poor fiber-matrix bond. This poor interfacial bond may have resulted in the radical difference of storage modulii observed in the uncoated and coated parts (see Figures 19 and 20). Although the results are promising, work is required to determine a more suitable separation layer material. Other paint formulations should also be evaluated.

3.2.3 Conclusion

In this experimental study, coinfusion was implemented. The resin and paint were coinfused between the flexible diaphragms. However, the separation layer did not perform as required, allowing the paint to seep through and mix with the resin. Material selection should continue to determine a more suitable separation layer material. Other paint formulation should also be evaluated in future work.

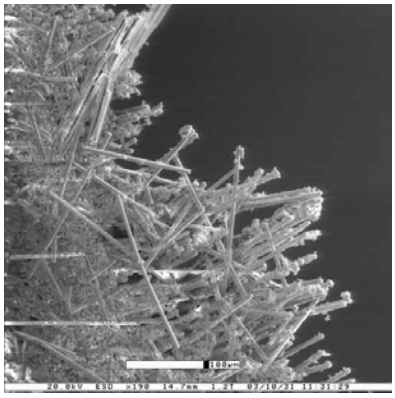

Figure 18. Microstructure of IMC RIDFTed component showing poor interfacial bonding.

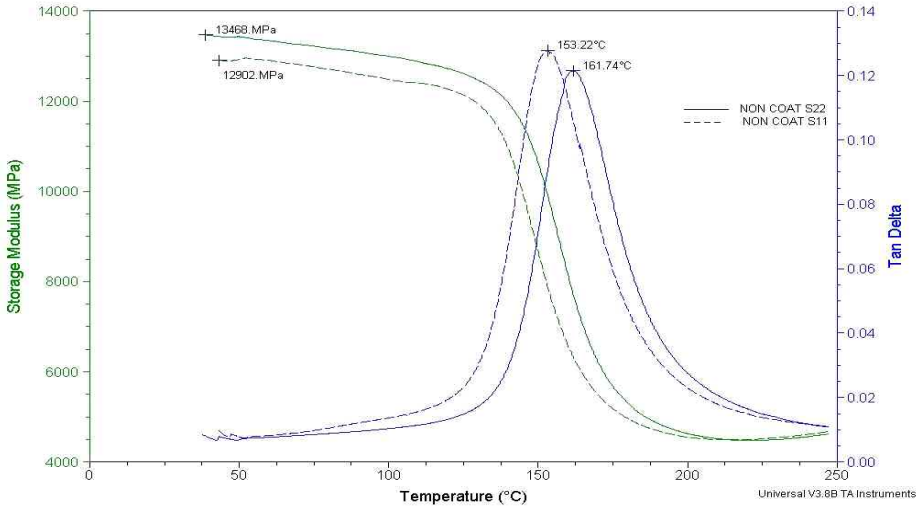

Figure 19. DMA diagram showing composite storage modulii for uncoated RIDFTed composite parts.

The ability to in-mold coat a composite will certainly advance its manufacturing. Nonetheless, the methodology for sustaining or improving mechanical properties and appearance of products should be the premise of implementing IMC. By applying IMC into the process today known as RIDFT, its unique approach to integrating flexible coatings with substrates is a natural fit for market segments such as automotive, agricultural, construction equipment, marine, lawn and garden, and aerospace.

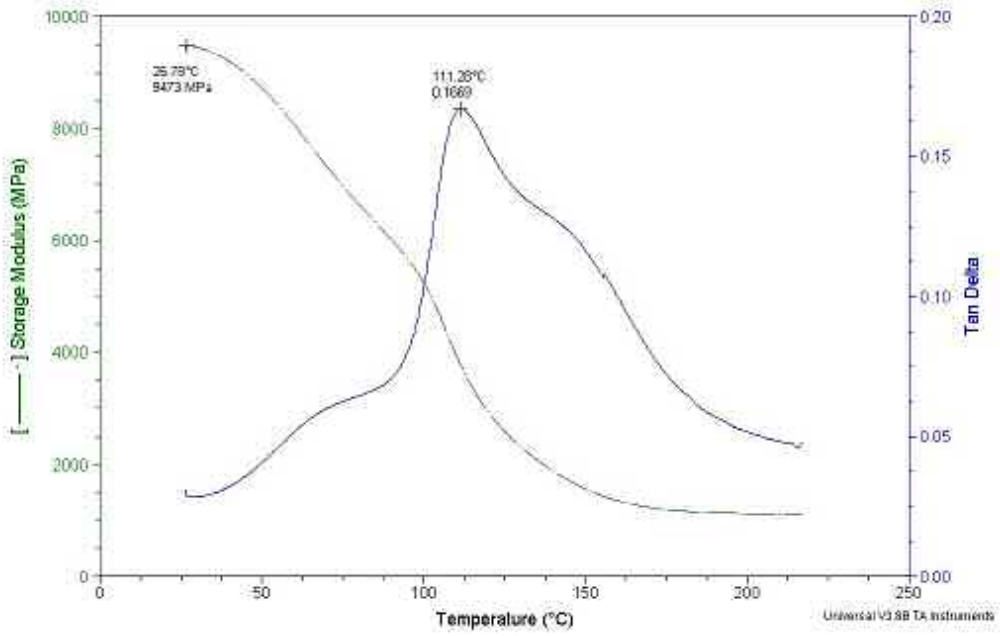

Figure 20. DMA diagram showing composite storage modulus for a coated, RIDFTed component.

This page intentionally left blank.

4. Implementation of UV Curing

The production cycle times of composite components largely depend on the time to cure. The ratio of the catalyst/resin mixture gives an estimate of the gelation and curing time, which determines the overall processing window for the manufacturing process. For room-temperature, cure-catalyzed resins, the time from gelation to cure can vary between one to three hours [7]. The composite part made would cure to sufficient demolding strength after twice the amount of time it took to gel the resin [7]. Consequently, a part that took one hour for the laminate to gel will require at least an additional two hours before it is ready to be demolded. This results in a manufacturing process that has a long production cycle time, in addition to an inflexible characteristic due to the restrictive nature of the processing window.

The ability to shorten the curing time will certainly enhance the compatibility of composites to the mass production sector. The RIDFT process was investigated with the view of shortening production cycle times by an alternative curing technique that involves the use of ultraviolet (UV) light.

4.1 Experimentation

4.1.1 Materials

The reinforcement material used for the experiments was a 7781 satin weave E-Glass fiber. The resin used was an epoxy based vinyl ester (Dera-kane 470-45). This resin was converted into a photoinitiated (light curing) resin by the addition of two classes of photoinitiators – the phenylbis (2,4,6-trimethylbenzoyl)-phosphine oxide (BAPO), and the alpha hydroxyl ketone oxide (AHK). The chemical structure of BAPO photoinitiator is shown in Figure 21.

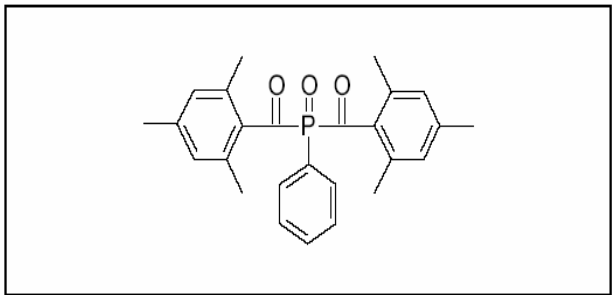

Figure 21. Chemical structure of Phenylbis (2,4,6 trimethylbenzoyl)-phenylphosphineoxide [8].

BAPO is a versatile photoinitiator used for radical photo polymerization of unsaturated resins upon exposure to UV light. It has demonstrated useful application in white-pigmented

formulations, the curing of glass fiber reinforced polyester/styrene systems, and clear-coats for outdoor use with light stabilizers [8].

The outstanding absorption properties of BAPO also allow for curing of thick sections. It can be used in combination with other photoinitiators, such as the alpha hydroxyl ketone oxide (AHK), as well.

4.1.1.1 Physical Properties of BAPO

1. Yellowish, powdery appearance at room temperature.

2. Melting point range of 127-133^{o}C.

3. Solubility at 20^{o}C(g/100g solution) in some monomer solutions is given in Table 3.

Table 3. Solubility of BAPO and AHK in monomer solutions

Photoinitiators	Acetone	Butyl Acetate	Methanol	Toluene
BAPO	14	6	3	22
AHK	>50	>50	>50	>50

The other class of photoinitiators used was the AHK. This is a highly efficient, non-yellowing photoinitiator, used to initiate the photopolymerisation of chemically unsaturated prepolymers in combination with mono or multifunctional vinyl monomers. The chemical structure of AHK is shown in Figure 22.

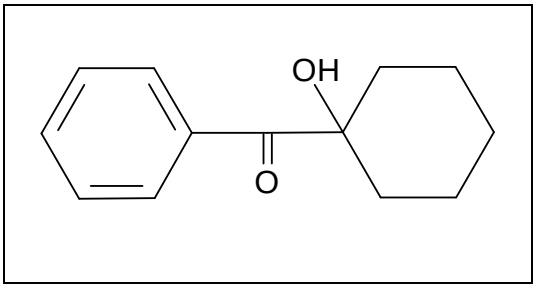

Figure 22. Chemical structure of alpha hydroxyl ketone photoinitiator [8].

4.1.1.2 Physical Properties of AHK

1. White to off-white crystalline powder appearance.

2. Melting point range of between 45-49^{o}C

3. Solubility at 20^{o}C (g/100g solution) in various monomer solutions is given in Table 3.

Both classes of photoinitiators can be used in combination with one another. The ratio of each photoinitiator mixed into the matrix is determined largely by the results required; this would include such component characteristics as surface finish quality, adhesion properties, and mechanical properties.

4.1.2 Preparation of Light-Curing Resins

As mentioned earlier, the resin used for the entire experiments was an epoxy-based vinyl ester resin. In order to make this resin light curable, photoinitiators were added in different proportions (%) of resin volume. The two classes of photoinitiators used for the experiments were BAPO and AHK. A measured quantity of resin, depending on the number of fiber layers, was poured into a 500 ml beaker that had been preweighed. The weight of the resin in the beaker was then measured and recorded. A predetermined quantity of 0.6% weight per hundred of resin (phr) for both classes of photoinitiators was measured unto two petri dishes. The photoinitiators were then mixed into the resin and stirred continuously until they were completely dissolved. For the experiments requiring a blend of both classes of photoinitiators, a mixture of both the BAPO and the AHK in the ratio of 1:3 for a total of 1.0 phr of resin content was used to produce the desired photoinitiated resin.

4.1.3 Fiber Preparation

The glass fabrics were cut into squares measuring 260 mm × 260 mm. The fibers were weighed using a digital measuring scale. Information about fiber weight was used to calculate the fiber volume fraction in each of the laminates. The dimensions of the fiber layers ensured that the laminates were large enough to produce sufficient specimen samples for the tensile and DMA tests. This was done to reduce or eliminate any anomaly that might arise with respect to the results obtained for each sample tested.

4.1.4 Design of the UV Stand

A stand for the UV lamp was constructed using a combination of stainless-steel angle iron, box tubing, and flat sheets. The angle iron was cut into two parts measuring 2 ft. × 2 ft. The box tubing was divided into four parts measuring 2 ft. in length, and two parts measuring 1ft. The stainless-steel plate was cut into two parts measuring 2 ft. × 2 ft. The two box tubing parts measuring 2 ft. served as the vertical stands through which the UV lamp could be lowered or raised. These were welded unto the angle irons. The flat steel plate was also welded unto the two remaining box tubings, which were used to connect both sets of angle irons. The entire setup (Figure 23) was mounted over the small RIDFT machine, as shown in Figure 24.

Figure 23. 3D schematic representation of the UV lamp support stand.

Figure 24. UV Lamp mounted over the RIDFT.

4.1.5 UV Experiments

The pre-cut layers of fiber were placed atop the bottom silicone membrane of the RIDFT. Flow paths were cut and placed at the infusion and the vacuum points. The top membrane was lowered into the setup and both membranes were sealed with the aid of a vacuum. Photoinitiated resin was then infused between the two silicone membranes. Once infusion was complete, aluminum foil was used to cover the resin infusion and the vacuum port rubber tubes to protect them from the intense UV light. The UV lamp position with respect to the distance from the surface of the top silicone membrane was then set in accordance to the design matrix. The UV lamp was turned on for the required duration of irradiation. The complete UV setup is shown in Figure 25.

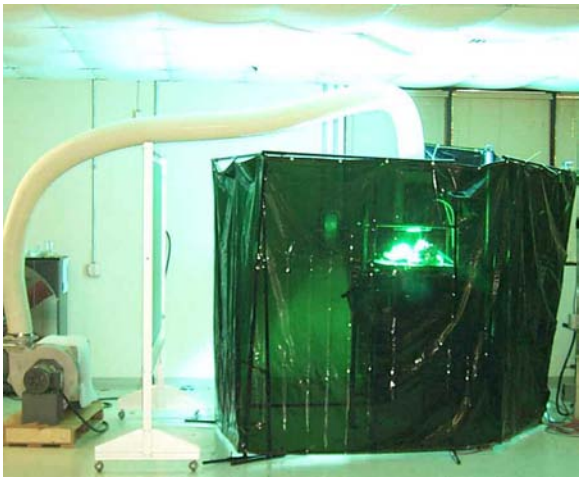

Figure 25. UV curing equipment in use.

Three sets of experiments were performed using a duration of irradiation of 60, 90, and 120 seconds. The experiments were timed using a digital stopwatch. The UV lamp was set at full power and placed 12 inches above the surface of the silicone membrane. After UV curing, the laminate was demolded from the RIDFT machine. Each laminate was weighed to ascertain the final weight of the composite, which would be used to calculate the fiber volume content in each laminate. The laminates were then prepared for tensile and thermal analysis testing.

4.1.6 Mechanical Testing and Material Characterization

Material property tests were performed on all laminates produced using a dynamic mechanical analyzer. These tests help determine the elastic properties of the composite laminates when subjected to sinusoidal loading. This gives an indication of the overall viscoelastic properties of each of the composite laminates. Values for both the storage modulus and glass transition temperatures (Tg) were obtained for each of the laminates, which helped facilitate the screening and comparison of the mechanical properties for each laminate produced.

Specimens for the DMA tests were produced by cutting out strips measuring 60 mm × 13 mm. The strips were positioned and clamped into place in the equipment as shown in Figure 26. Each laminate was heated at a constant rate and deformed (oscillated) at constant amplitude (strain) of 10.0 mm and frequency of 1 Hz. A ramp rate of 5^{o}C/minute for a final temperature of 250^{o}C was used, resulting in a total run time of 50 minutes.

Tensile tests were performed on each of the laminates. These tests were carried out in accordance with the ASTM 3039 standards [9]. Specimens for the tensile test were produced by cutting out laminate strips measuring 200 mm × 25 mm. The specimens were cut 3 mm oversize and final dimensions obtained by grinding. Aluminum end tabs 3.2 mm thick and measuring 50 mm × 25 mm were locally bonded onto both ends of each laminate using Epon 562 resin in conjunction with a 105 hardener. This resulted in a gage section of 100 mm (Figure 27).

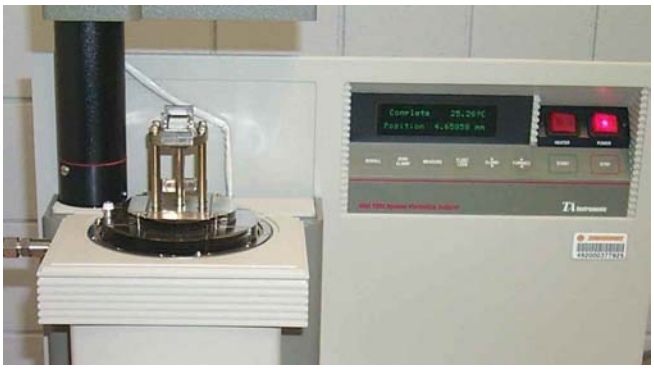

Figure 26. Composite specimen mounted on DMA machine in preparation for testing.

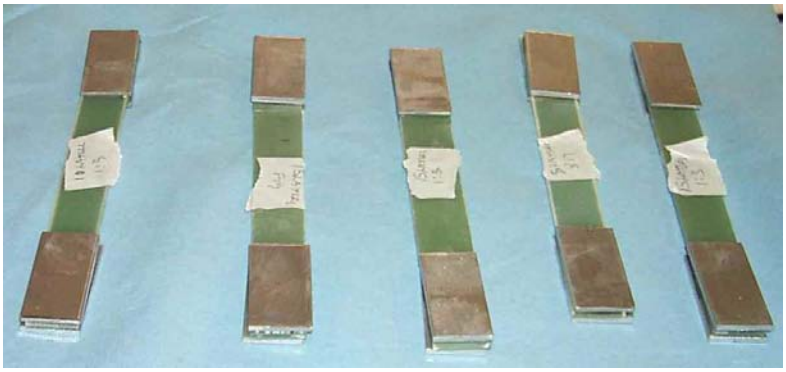

Figure 27. Tensile test specimens.

Six specimen strips were cut from each of the composite laminates. Each specimen strip was placed between the grips of two load cells of an MTS Systems tensile testing machine, as shown in Figure 28. An extensometer was used to measure strain from the experiments. The test specimens were held so that sufficient lateral pressure was applied to prevent slippage between the grip face and tabs. The tensile tests were carried out at a crosshead separation rate of 2 mm per minute.

4.2 Results and Discussion

4.2.1 DMA (Dynamic Mechanical Analysis) Results

Three separate sets of DMA experiments were carried out using a duration of irradiation of 60, 90, and 120 seconds. The goal was to determine if UV-cured laminates could be produced with consistent material properties for each case, as well as to determine what effect, if any, an increase or decrease in the duration of irradiation would have on the overall material properties for each of the UV cured laminates. DMA results for each set of experiments are shown in Figures 28 to 31.

Figure 28. Setup for the tensile testing of composite laminates.

Examination of the DMA plot in Figure 29 for the UV laminate cured for 60 seconds shows that both samples tested produced similar results with respect to the Tg and the storage modulus. However, the plot does reveal an almost instantaneous decline in the storage modulus of the composite laminate right from the onset of testing. This invariably implies that the laminate experiences an instant decline in its viscoelastic properties once subjected to sinusoidal loading. This may have resulted from inadequate crosslinking of the functional groups in the thermoset (vinylester molecules) brought on by an incomplete curing reaction.

The DMA plot for the UV composite laminate cured for 90 seconds (Figure 30) shows that both samples produced consistent Tg and storage modulus values. However, in contrast to the results obtained for the laminate cured for only 60 seconds, these laminates did not experience an immediate decline in storage modulus when subjected to sinusoidal loading. This probably indicates that the laminates have been cured to a better degree when exposed to an irradiation time of 90 seconds under the UV lamp.

Similar to what was obtained in the two previous plots, the UV laminates cured for 120 seconds produced consistent material properties, as shown in Figure 31. The laminates do not appear to lose their viscoelastic properties immediately once subjected to sinusoidal loading.

Figure 32 shows the DMA results for a laminate that was cured using MEKP and an infrared heat lamp for 30 minutes. The material properties for the two samples appear consistent with regards to the storage modulus and the glass transition temperature. The plot also shows that the composite laminates undergo a steady decline in its viscoelastic properties when subjected to sinusoidal loading, as evidenced by the steady decline in the storage modulus value. A summary of the DMA results is given in Table 4.

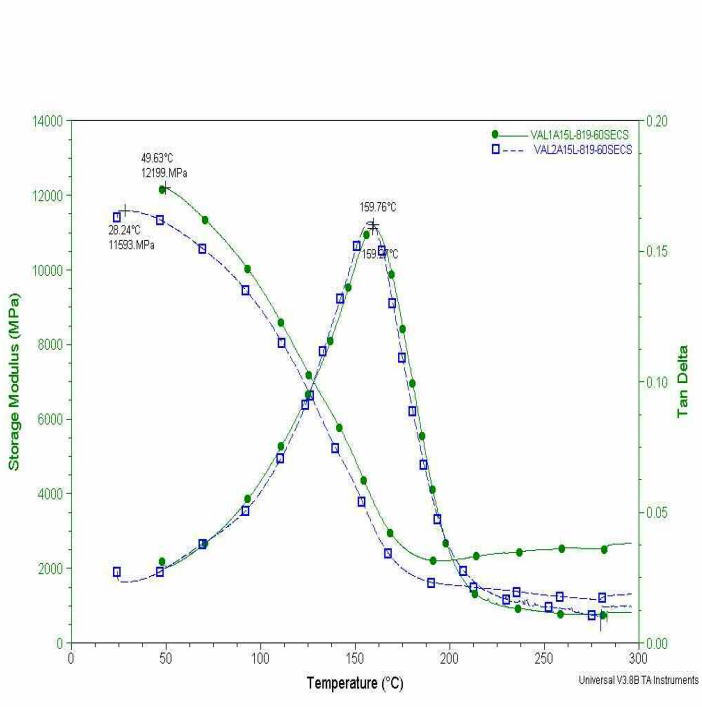

Figure 29. DMA Results for UV laminates cured for 60 seconds.

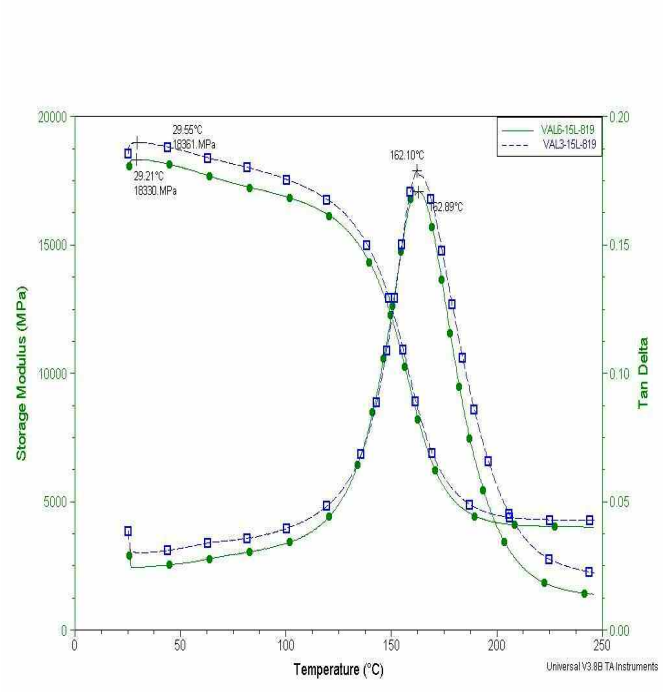

Figure 30. DMA Results for UV laminates cured for 90 seconds.

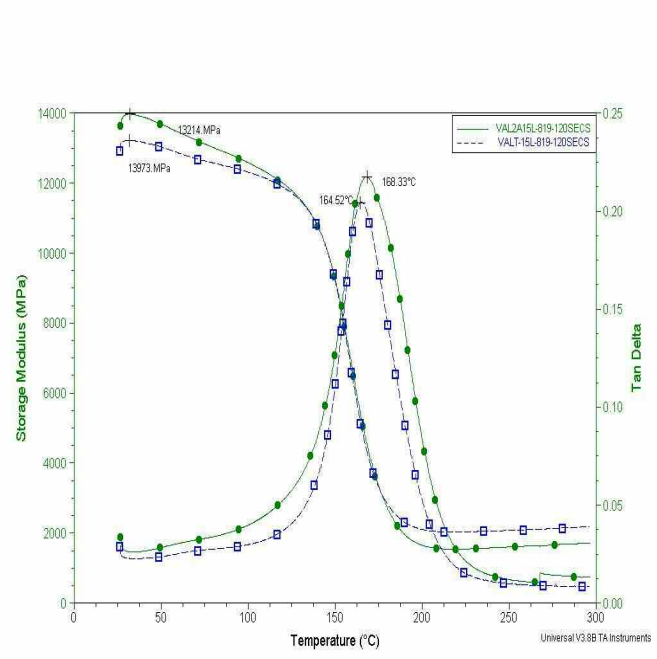

Figure 31. DMA Results for UV laminates cured for 120 seconds.

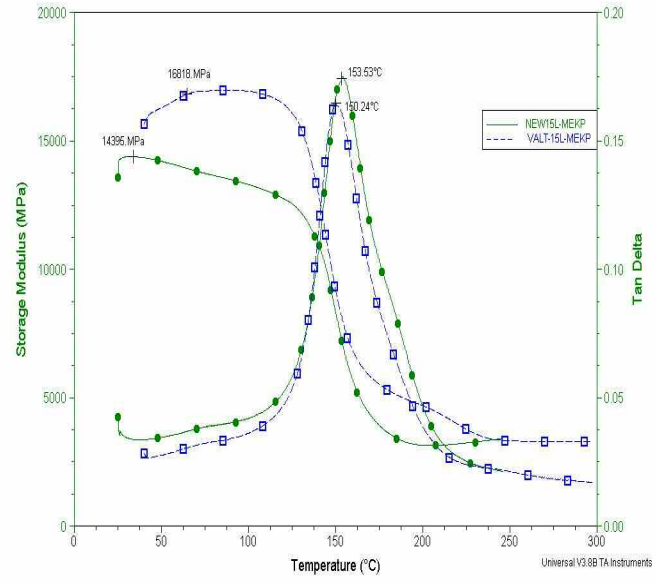

Figure 32. DMA Results for laminates cured using MEKP Catalyst.

The results shown in Table 4 indicate that the most favorable results with regards to both the storage modulus and the Tg were obtained from the laminates cured using UV light for 90

Table 4. Summary of DMA results (laminates with 15 layers of glass).

Experiment	Duration of Irradiation	Storage Modulus (MPa)	Tg (°C)
1-UV	60 s	11593	159.76
2-UV	60 s	12199	159.26
3-UV	90 s	18361	162.10
4-UV	90 s	18330	162.89
5-UV	120 s	13970	165.70
6-UV	120 s	13155	167.29
7-MEKP	30 min	14395	153.53
8-MEKP	30 min	16818	150.24

seconds. Increasing the irradiation time from 90 to 120 seconds resulted in a 24% decrease in storage modulus (Figure 33). This suggests that the extra 30 seconds provides excessive irradiation, which may be detrimental to the cured laminate. The lower storage modulus value, as well as the shape of the curve for the DMA plot (Figure 29) obtained for UV laminates cured for 60 seconds, may be attributed to incomplete curing of the laminates, which made it undergo an instant decline in its material properties during the DMA test. Conversely, the DMA plots for the UV laminates cured for 90 seconds and 120 seconds, as well as the MEKP cured laminates, show a steady decline in storage modulus during DMA testing. This supports the earlier postulation that an incomplete (polymerization) curing reaction was the most likely reason behind the immediate loss of material properties in the UV laminates cured for 60 seconds.

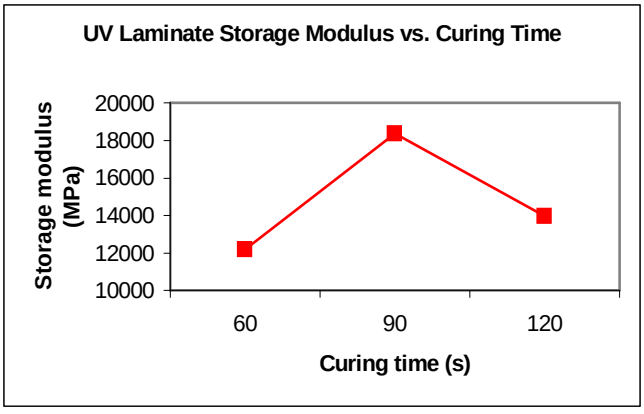

Figure 33. Laminate storage modulus versus UV curing time.

4.2.2 Tensile Properties

The DMA material property tests performed earlier indicated that the UV laminates cured for 90 seconds had the best properties with regards to both the storage modulus and Tg. As a follow up, two separate sets of tensile test experiments were carried out using three different samples of a UV composite laminate that was cured for 90 seconds, as well as three different samples for an MEKP-cured thermal laminate. The tensile test results are given in Table 5.

Table 5. Tensile test results (15 layers of glass – 40% V_f).

Setup	Tensile Strength (MPa)	Young's Modulus (GPa)
1-UV	319.41	28.89
2-UV	315.47	27.39
3-UV	320.62	28.34
4-MEKP	318.46	15.81
5-MEKP	306.62	12.74
6-MEKP	316.19	14.74

The plot in Figure 34 shows that there is no statistically significant difference in the tensile strength for both the UV-cured and the MEKP laminates as evidenced by the overlapping error bars. However, there does appear to be a statistical difference in the tensile modulus for both sets of laminates, with the UV-cured laminates having a greater value (83%), as shown in Figure 35. McCarthey [10], in his UV cocooning experiments, demonstrated that UV curing helps to trap styrene molecules that would ordinarily have been lost through evaporation, making them available to help drive the polymerization curing reaction. This may have been responsible for the improved tensile modulus results obtained for the UV-cured laminates.

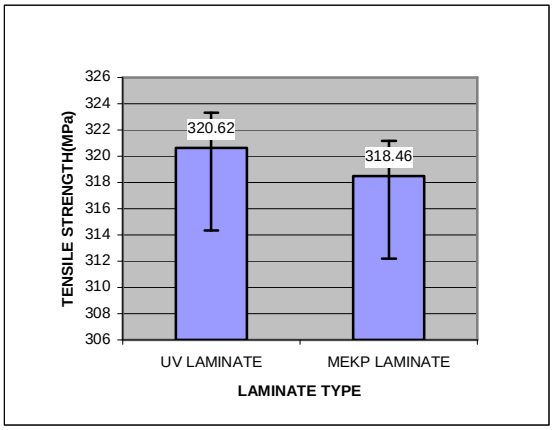

Figure 34. Tensile strength versus laminate type.

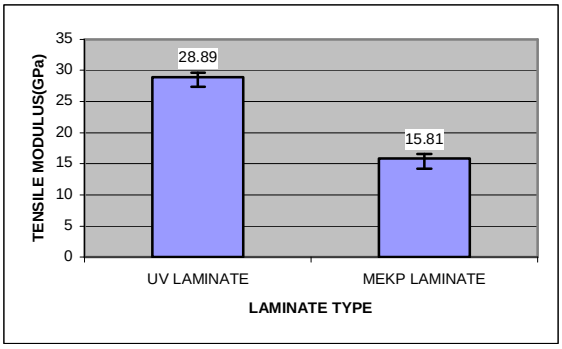

Figure 35. Tensile modulus versus laminate type.

4.2.3 Microstructural Study

In addition to mechanical and material property tests, an Environmental Scanning Electron Microscope (ESEM) was used to examine the microstructure of the UV-cured laminates and the thermally-cured MEKP-based laminates. The objective was to determine if proper adhesion and fiber wet-out occurred in each of the laminates.

The ESEM micrograph for a UV-cured laminate in Figure 36 shows that good fiber wet-out was achieved in the laminates. This is critical for any composite laminate, because the matrix acts as the load transfer medium in the laminate, enabling the composite to achieve its full mechanical strength under service conditions. Figure 37 also shows a UV-cured laminate. Good adhesion between the matrix and the fibers can be observed from the bunched fiber segments. Figure 38 shows a damaged section of a MEKP-cured laminate. The visible fragmented matrix sections are indicative of a good fiber-matrix bonding.

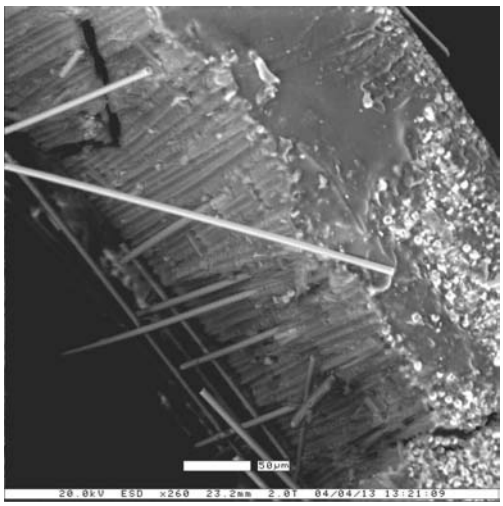

Figure 36. ESEM micrograph of a UV-cured laminate showing good fiber wet out.

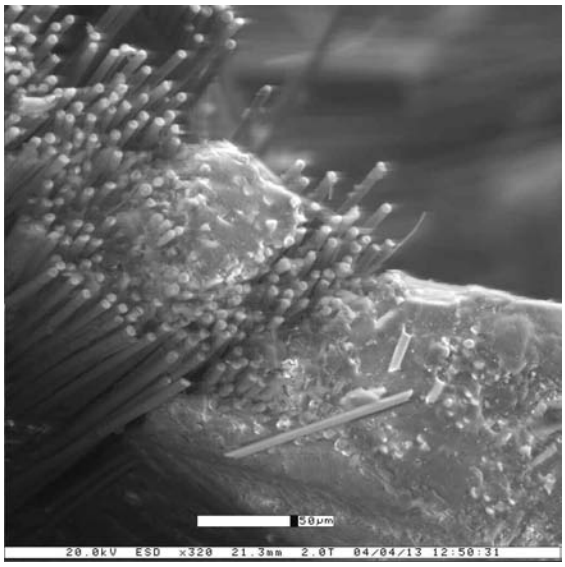

Figure 37. ESEM micrograph of a UV-cured laminate showing good fiber-matrix adhesion.

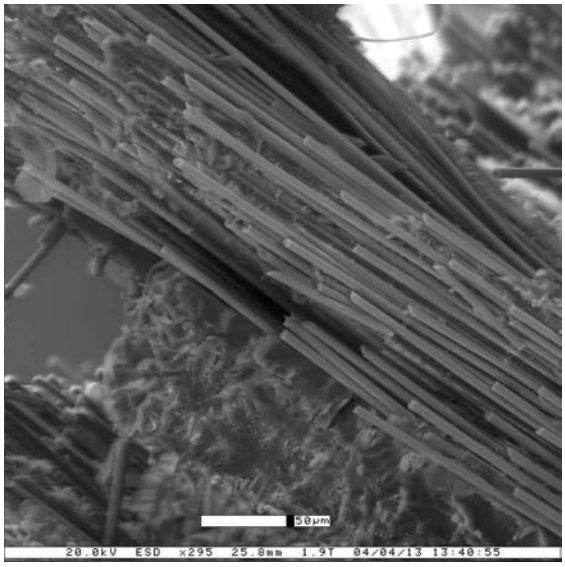

Figure 38. ESEM micrograph of a thermally-cured laminate.

4.3 Conclusion

This work successfully incorporated a UV curing system to the RIDFT process. The resulting UV laminates not only exhibited consistent mechanical and thermal mechanical properties, but also had properties that were comparable to thermally cured composite laminates made using the same settings.

Experiments were performed that determined the best exposure time was 90 seconds. A shorter time (60 s) resulted in incomplete curing, and a longer time (120 s) resulted in laminates with inferior properties.

A comparison was made between the tensile properties of the UV-cured and the MEKP-cured laminates. No significant differences were found between the tensile strengths of the UV-cured (90s) and the MEKP-cured laminates. However, the Young's modulus differed considerably between the two. The UV laminates had a higher Young's modulus (83%) than the MEKP laminates. A comparison of the cure times yielded a factor of 20:1 in favor of UV curing (based on a curing time of 90 s).

The radiometric measurements of some critical process design requirements need to be studied in future work. Some of these parameters include peak and focus irradiance, which is characteristic of the different types of reflectors used in the lamp, spectral distribution, and energy dose with temperature and time. Radiometric measurements would be critical in quantifying the successful exposure parameters so the cure on demand process could be readily duplicated.

Further research should determine the effects of the silicone membrane on the actual UV energy dose getting to the substrate, establishing the optimal lamp settings unique to the RIDFT process with respect to the type, nature of bulb, and reflector cavity used in the UV lamp. This would invariably help improve the overall efficiency by determining the exact form of wavelength and levels of irradiance that would reduce the total energy delivered to the membrane while still accomplishing complete cure.

5. Summary of Findings

In the duration of the sponsored research work, developmental work was carried out to enhance the capabilities of the RIDFT process. In-mold coating was investigated as a methodology for the painting of composite components manufactured by the RIDFT process. Paint films were implemented with promising results. Due to the morphology of the paint films assessed, problems occurred with adhesion. As such, it was suggested that films with better adhesion characteristics should be assessed. Such a film is the GE Lexan material. Another methodology was sort for in-mold coating, which involved the coinfusion of two fluids into the mold. In this case, the coinfusion was shown to be viable; however, a suitable separation material needs to be used to prevent the premature mixing of the two fluids. Another approach may be the formulation of coating materials that will better interact with the FERRO #MCO8 Prepak™ material.

This work also investigated the utilization of UV lamps to cure photoinitiated resin during the RIDFT process. The idea was to take advantage of the translucent nature of the silicone diaphragms used in the RIDFT process. UV curing was successfully implemented, reducing curing times by a factor of 20 compared with thermal curing, whilst improving the mechanical properties of the resulting components.

This page intentionally left blank.

6. References

1. J.R. Thagard, O.I. Okoli, Z. Liang, H-P Wang, C. Zhang. 2003. "Resin Infusion between Double Flexible Tooling: Prototype Development," *Composites: Part A* 34, (pp. 803–811).

2. J.R. Thagard, O.I. Okoli, Z. Liang, "Resin Infusion between Double Flexible Tooling: Evaluation of Process Parameters," *JRPC (in print)*.

3. "Colourful Times in the Coatings Industry," 2003. *Automotive Industry Agenda*, Sterling Publications, (pp.119-121).

4. R. Haglund. 1998. *In-Mold Top Coating on Automotive Exterior SMC Panels.* Thesis, Lund Institute of Technology, 39.

5. E.J. Straus, D. McBain, and F. Wilczek. 1997. *Reinforced Plastics*, 41.

6. E. F. Gillio, S. G. Advani, J. W. Gillespie Jr. 1998. "Investigation of The Role of Transverse Flow In Co-Injection Resin Transfer Molding," *Polymer Composites*. 19(6), (pp.738-746).

7. M. Livesay. *Low Cost Manufacturing Processes using UV Cure Resins*. Proc. Composites '97 Manufacturing & Tooling Conference, January 1997.

8. Ciba Specialty Chemicals. 2001. *Chemical Structure and Properties of Irgacure 184 and Irgacure 819*, 4th edition.

9. *Annual Book of ASTM Standards*, 2000. Section 3, Volume 03.01.

10. R. McCartney. "Composite UV Cocooning." Rad-Tech Report, May/June 2001.

This page intentionally left blank.

DISTRIBUTION:

1 MS 0964 Heidi Ruffner, 05731
1 0511 Carol Adkins, 01020
1 0959 Bob Poole, 14152
1 0101 Paul Robinson, 00001
1 0958 Mike Kelly, 14153
1 0958 Jeff Galloway, 14153
1 0958 John Emerson, 14153
1 0123 Marie Garcia, 01010

1 MS 0123 LDRD Office, Donna Chavez, 01011

1 Dr. O. I. Okoli
Dept. of Industrial & Mfg. Engineering
FAMU-FSU College of Engineering
2525 Pottsdamer Street
Tallahassee, FL 32310-6046

1 MS 9018 Central Technical Files, 08945-1
2 0899 Technical Library, 09616